Notes regarding the coupling of a z-oriented dipole emitter to a nanofiber based photonic crystal cavity

Mark Sadgrove[1]

[1] *Center for Photonic Innovations, The University of Electro-Communications, 1-5-1 Chofugaoka, Tokyo, Japan*

Two aspects of the coupling of dipole emitters to nanofiber based photonic crystal cavities appear strange at first sight: namely (1) The fact that the position dependent coupling strength of the z-dipole varies in opposite phase to that of transversely oriented dipoles and (2) the fact that the coupling for the z-dipole is of the same order as that for transverse oriented dipoles despite the usual intuition that the z components of the nanofiber guided mode is small relative to the transverse components. Here, we will show that these features of the z-dipole coupling are simple consequences of the nature of the hybrid fundamental mode of the nanofiber. Furthermore, these results suggest two unique features of our work compared to NV center or other schemes where the quantum emitters are embedded in the bulk: (A) The z component coupling is significant in our case *because* the emitters are on the surface of the fiber where the z-component is non-negligible and (B) the fiber axis position averaged coupling for a randomly oriented dipole emitter is larger than expected because the z-polarized cavity mode is 180 degrees out of phase compared with the transverse components, *allowing significant coupling to occur, even if the emitter is not perfectly aligned with the cavity center.*

I. BACKGROUND

Finite difference time domain simulations for a dipole emitter on the surface of a photonic crystal (PhC) nanofiber can be used to find the variation in the cavity enhancement of spontaneous emission as a function of displacement from the cavity centre. A surprising aspect of the results of such simulations is that a z-oriented dipole experiences zero coupling to the guided modes at the cavity centre, but steadily increases in coupling as the displacement from the cavity increases until it reaches a maximum just as the transversely-oriented dipole experiences a minimum. Furthermore, the coupling of the z component at the maximum point is less than but of the same order as the coupling of transversely-oriented dipoles.

Below, we will explain these observations from simulation results in terms of analytical results for Purcell enhancement and the hybrid modes of a nanofiber. We will assume a single mode fiber in all cases for simplicity. In particular we will use the following facts:

1. A given dipole orientation couples to modes with the same polarization orientation, e.g. a y-oriented dipole couples to the y-polarized fundamental mode, an x-polarized dipole couples to the x-polarized fundamental mode and the z-dipole orientation can couple to either of x or y polarized fundamental modes, since both have z components.

2. The coupling or enhancement of spontaneous emission for an emitter at a given position r in the cavity is proportional to the field intensity with the relevant polarization at the position r.

3. The guided modes of a single mode fiber are either x or y polarized hybrid HE_{11} modes.

4. The z-polarized component of the hybrid modes HE_{11} is phase shifted by $\pi/2$ with respect to the transverse polarizedcomponent of the mode.

5. The z-component of the hybrid modes HE_{11} has a minimum at the fiber center and is maximal at the fiber surface

These five facts explain the two observations regarding coupling of a z-oriented dipole as given in the abstract. we now proceed to present the above-listed facts in more detail.

II. THEORY OF COUPLING OF A DIPOLE EMITTER TO A PHOTONIC CRYSTAL CAVITY

we will not present a detailed review of the theory of coupling between emitters and PhC cavities here. we refer the reader to the 101st Les Houches Summer School lectures given by Jelena Vuckovic [1]. The material we present here is taken directly from these lecture notes, and a full derivation can be found in [1].

Here we are interested in the variation of coupling of the dipole to the PhC nanofiber as a function of the position of the dipole along the fiber axis. Physically, the dipole source is assumed to be a two level system with resonant frequency ω_0, but in simulations, the field is simply a classical dipole source characterised by a dipole emitter strength. There is no particular need to use quantum expressions in the present treatment.

We introduce the following parameters to characterize the dipole emitter and the field. In all cases, bold-face variables represent vector quantities, while non-bold variables are always scalars.

- $\boldsymbol{\mu}_d$ is the dipole moment. As an example, in the case of a one-electron, two level atom, with ground and excited states $|g\rangle$ and $|e\rangle$ respectively, it is given by the matrix element $\boldsymbol{\mu}_d = \langle g|q_e\mathbf{d}|e\rangle$ where q_e is

the elementary charge, and $\mathbf{d}$ is the position of the electron relative to the nucleus.

- $\mathbf{r}_d$ denotes the position of the dipole emitter.
- $E(\mathbf{r})$ is the *scalar* electric field whose direction is given by the following prameter.
- $\mathbf{p}(\mathbf{r})$ is the polarization of the electric field at position $\mathbf{r}$.
- V_c is the cavity mode volume.
- $n(\mathbf{r})$ is the refractive index.
- $\mathbf{r}_M$ denotes the position of the maximum of the field in the cavity.

We use these defintions in the following expressions for the coupling of a dipole emitter to a cavity mode. It may

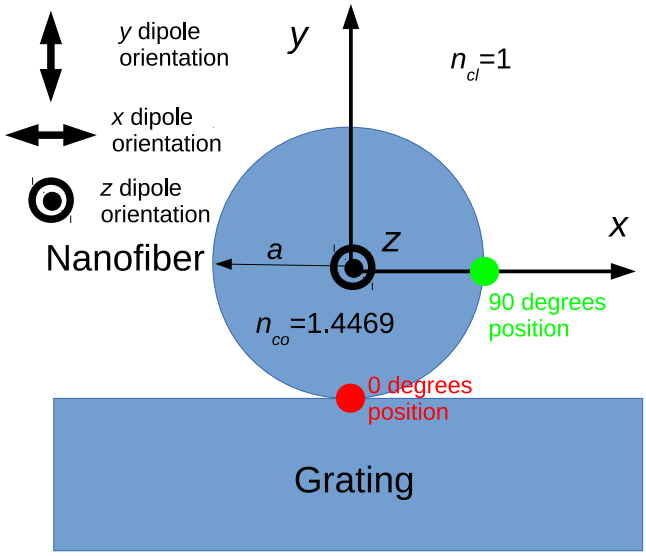

FIG. 1. Schematic diagram of the system which we consider. A silica nanofiber ($n = 1.4469$) is mounted on a silica grating cavity. Dipole emitters with the shwon orientations can be placed on the surface of the nanofiber, typically at the 0 degree position (red dot) or the 90 degree position (green dot).

be shown that position dependent coupling factor $g(\mathbf{r})$ between the dipole emitter and the cavity at the position $\mathbf{r}$ as measured from the cavity center is [1]:

$$g(\mathbf{r}) = g_0 \psi(\mathbf{r}) \cos(\eta), \tag{1}$$

where

$$g_0 = \frac{\mu_{eg}}{\hbar}\sqrt{\frac{\hbar\omega_0}{2n^2(\mathbf{r}_M)V_c}}, \tag{2}$$

$$\psi(\mathbf{r}) = \frac{E(\mathbf{r}_d)}{|E(\mathbf{r}_M)|}, \tag{3}$$

and

$$\cos(\eta) = \frac{\boldsymbol{\mu}_d \cdot \mathbf{p}(\mathbf{r}_d)}{|\boldsymbol{\mu}_d|}, \tag{4}$$

where η is the angle between the vectors $\boldsymbol{\mu}_d$ and $\mathbf{p}(\mathbf{r}_d)$.

In [1], Vuckovic goes on to show that the Purcell factor may be written in terms of the coupling g given above, the cavity spectral halfwidth κ and the natural decay rate Γ_0 as

$$F_P = \frac{2|g|^2}{n_{\text{eff}}\Gamma_0\kappa}. \tag{5}$$

where n_{eff} is the effective refractive index of the cavity medium.

For the purposes of calculating enhancements, which we are interested in here, the dipole strength g_0 is arbitrary and may be set to any constant value. The terms that we are interested in are $\psi(\mathbf{r})$ which governs how the coupling of the dipole changes with its position in the cavity and $\cos(\eta)$ which tells us that there is only coupling between the dipole and the cavity when the dipole moment is aligned with the field polarization.

III. RELEVANT PROPERTIES OF THE HYBRID FUNDAMENTAL MODE OF A NANOFIBER

Having seen how the coupling of a dipole emitter to a cavity depends on the cavity field, we now consider the form of the field in our PhC nanofiber cavities. We will assume that the perturbation caused by the index modulation (caused by an external grating or periodic nanocraters) is small enough that the propagating modes are well described by the fundamental HE_11 hybrid mode. Let us review the form of these modes, using expressions found in Okamoto [2]. We assume that all modes have the form $\mathbf{E}(\mathbf{r},t) = \mathbf{E}(\mathbf{r})\exp(\text{i}(\omega t - \beta z))$. The wavelength of the field is taken to be λ and the wavenumber is $k = 2\pi/\lambda$. For a fiber of radius a, with core rfractive index n_{co} and cladding refractive index n_{cl}, the eigenvalue equation which allows the propagation constant β to be found is

$$\left[\frac{J_n'(U)}{UJ_n(U)} + \frac{K_n'(u)}{WK_n(W)}\right]\left[\frac{J_n'(U)}{UJ_n(U)} + \left(\frac{n_{\text{cl}}}{n_{\text{co}}}\right)^2\frac{K_n'(u)}{WK_n(W)}\right] = n^2\left(\frac{1}{U^2}+\frac{1}{W^2}\right)\left[\frac{1}{U^2}+\left(\frac{n_{\text{cl}}}{n_{\text{co}}}\right)^2\frac{1}{W^2}\right], \tag{6}$$

where $U = a\sqrt{k^2 n_{\rm co}^2 - \beta^2}$ and $W = a\sqrt{\beta^2 - k^2 n_{\rm cl}^2}$

For the HE_{11} mode (i.e. taking the lowest spatial frequency solution for $n = 1$ in the eigenvalue equation), the components of $\mathbf{E}(\mathbf{r})$ in cylindrical polar coordinates where $\mathbf{r} = (r, \theta, z)$ are [2]

$$E_r = -\mathrm{i}\frac{\beta a}{U}\left(\frac{1-s}{2}J_0(U/ar) - \frac{1+s}{2}J_2(U/ar)\right)\cos(\theta+\psi), \tag{7}$$

$$E_\theta = \mathrm{i}\frac{\beta a}{U}\left(\frac{1-s}{2}J_0(U/ar) + \frac{1+s}{2}J_2(U/ar)\right)\sin(\theta+\psi), \tag{8}$$

$$E_z = J_1(U/ar)\cos(\theta+\psi). \tag{9}$$

for $r \leq a$ and

$$E_r = -\mathrm{i}\beta a\frac{J_1(U)}{WK_1(W)}\left(\frac{1-s}{2}K_0(W/ar) + \frac{1+s}{2}K_2(W/ar)\right)\cos(\theta+\psi), \tag{10}$$

$$E_\theta = \mathrm{i}\beta a\frac{J_1(U))}{(WK_1(W)}\left(\frac{1-s}{2}K_0(W/ar) - \frac{1+s}{2}K_2(W/ar)\right)\sin(\theta+\psi), \tag{11}$$

$$E_z = \frac{J_1(U)}{K_1(W)}K_1(W/ar)\cos(\theta+\psi). \tag{12}$$

for $r > a$. Note that $J_n(x)$ is a Bessel function of the first kind and $K_n(x)$ is a modified Bessel function of the second kind. Additionally we note that two degenerate polarizations are defined by the above equations - the x polarization denoted HE_{11}^x where $\psi = 0$ and the y polarization denoted HE_{11}^y where $\psi = \pi/2$. We can convert to cartesian field components using the transformation

$$E_x = E_r\cos(\theta) - E_\theta\sin(\theta), \tag{13}$$

$$E_y = E_r\sin(\theta) + E_\theta\cos(\theta). \tag{14}$$

Although we have used the formalism found in Okamoto [2] here, we have compared the results obtained using the slightly different formalism found in, e.g., Le Kien *et al.* [3] and checked that the results are the same.

In the real experiment, the circular symmetry is broken by the grating as shown in Fig. 1, but we will assume that the modes in the nanofiber are still well approximated by the x and y polarized HE_{11} modes. In the following we will focus on just the HE_{11}^y mode since the physics of dipole emitter coupling to either mode is the same. We will fix the parameters as follows: $a = 300$ nm, $\lambda = 800$ nm. Solving the eigenvalue equation for these parameters gives $U \approx 0.8151$, $W \approx 1.6811$ and $\beta/k \approx 1.2284$.

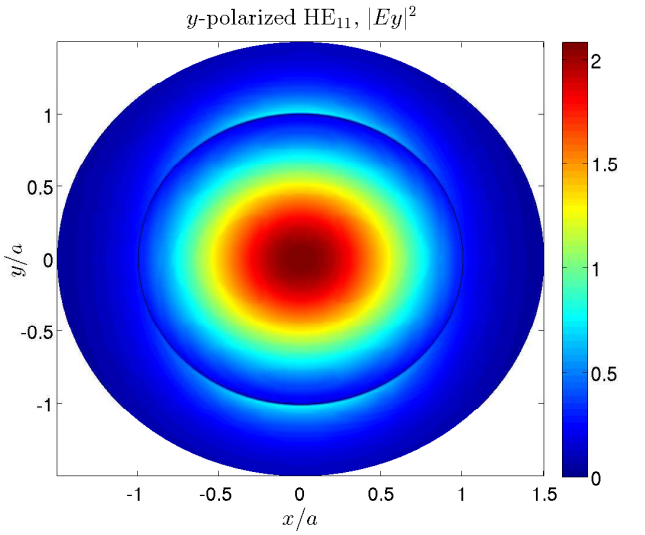

FIG. 2. Intensity of the y components of HE_{11}^y. The black circle indicates the fiber surface.

A. Position dependence of coupling in the $x-y$ plane

Keeping in mind the coupling theory outlined in Section II, we can use the intensity profiles shown in Figs. 2, 3, and 4 for the HE_{11}^ymodes to make some general observations about coupling of dipole emitters to the

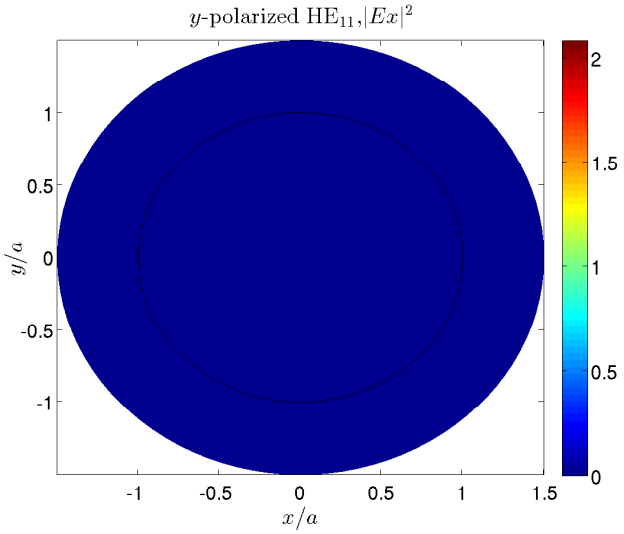

FIG. 3. Intensity of the x components of HE_{11}^{y}.

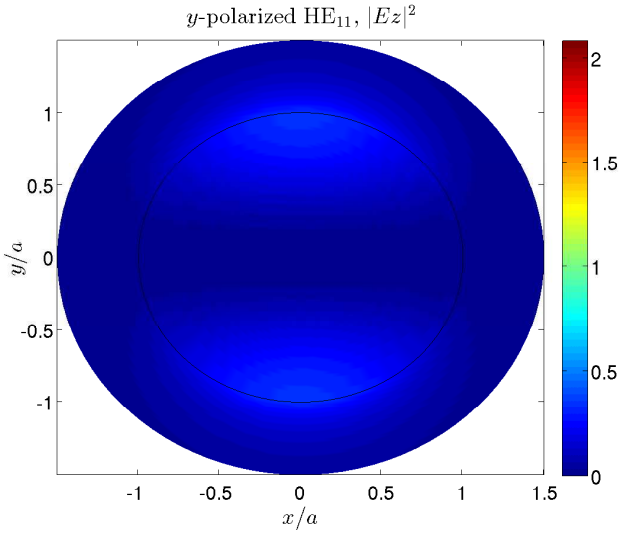

FIG. 4. Intensity of the z components of HE_{11}^{y}.

PhC nanofiber. The facts which we need are: (1) an α-polarized emitter, where $\alpha \in \{z, y, z\}$ couples only to the α-polarized component of the fiber mode and (2) the coupling is proportional to the field strength.

For example, in the case of the zero degree position (see Fig. 1), a y-polarized dipole at the surface of the fiber ($x = 0$,$y = a$) couples maximally to the HE_{11}^{y}mode relative to any other azimuthal position modulo 180 degrees. The minimum coupling is seen to occur at the 90 degree position ($x = \pm a$,$y = 0$), but we note that the coupling is still non-zero even at this position.

Similarly because the x-polarized component of the HE_{11}^{y}mode is negligible (Fig. 3) the coupling of an x-polarized dipole emitter to the HE_{11}^{y}mode is also negligible for *any* position.

In the case of a z-polarized dipole, coupling is strongest

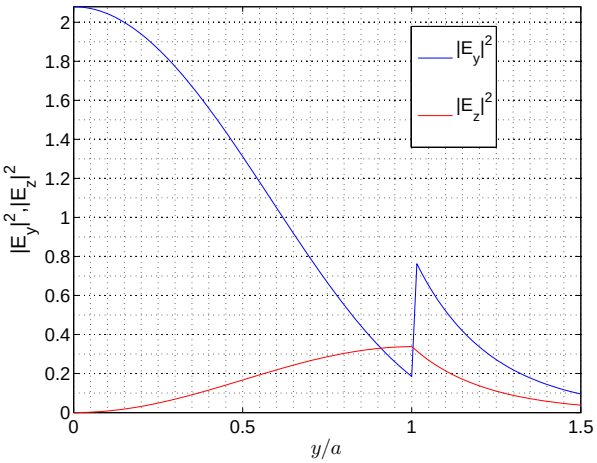

FIG. 5. Comparison of intensities for the $\mathrm{HE}_{11}^{y}y$ and z components along the y axis.

	HE_{11}^{y}			HEx11		
Dipole orientation	x	y	z	x	y	z
Zero degree placement	0	max	max	min	0	0
90 degree placement	0	min	0	max	0	max

TABLE I. Couplings for each dipole orientation to the $\mathrm{HE}_{11}^{x}$and HE_{11}^{y}modes for 0 and 90 degree dipole placements.

at the 0 degree position ($x = 0$,$y = a$) as for a y-polarized emitter. However, for the 90 degree position, the coupling vanishes unlike the case for a y-polarized emitter where coupling is minimal but non-zero.

Table III A summarizes the coupling between dipole emitters and the guided modes. (Note that the field modes for $\mathrm{HE}_{11}^{x}$are shown in the appendix).

Finally, Fig. 5 shows the variation of the intensities of the non-vanishing components of HE_{11}^{y}i.e. $|E_y|^2$ and $|E_z|^2$ along the y-axis. It is clear that the contribution from the z axis is maximal at the fiber surface (where the emitters are placed in our experiments) and tends to near the fiber center. This suggests that our experiment is uniquely suited to take advantage of the z-dipole emitter coupling compared to experiments, e.g. using NV centers, where the emitter is in the bulk. For such experiments, the z component of the mode at the emitter position can be assumed to be small, but in our case the opposite is true.

B. Standing wave of the HE_{11}mode - transverse and longitudinal components are in anti-phase

In the cavity, the HE_{11}mode is reflected and its counterpropagating partner is therefore also present. Therefore it is the HE_{11}standing wave that we must consider if we wish to understand the coupling of a dipole emitter to the cavity field. On reflection, we expect the complex amplitude of each component to be rotated by 180 de-

grees. This is the same as subtracting the conjugate of each component. Therefore, the equations for the standing wave components of the HE_{11}modes is

$$E_x^s = E_x \exp(-\mathrm{i}\beta z) - E_x^* \exp(\mathrm{i}\beta z) \quad (15)$$
$$E_y^s = E_y \exp(-\mathrm{i}\beta z) - E_y^* \exp(\mathrm{i}\beta z) \quad (16)$$
$$E_z^s = E_z \exp(-\mathrm{i}\beta z) - E_z^* \exp(\mathrm{i}\beta z). \quad (17)$$

where * denotes the complex conjugate.

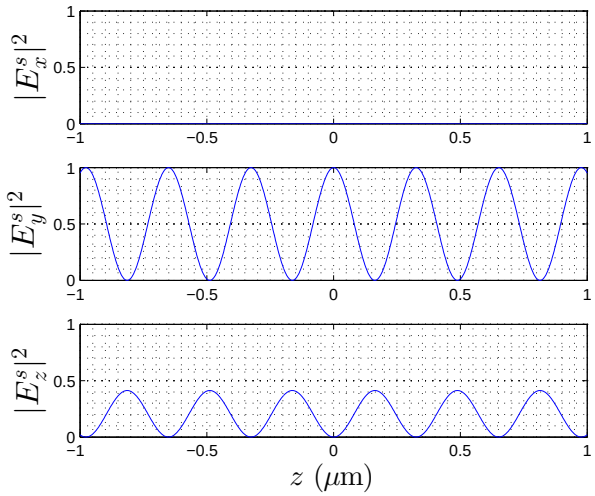

FIG. 6. Intensity of the y components of HE_{11}^x. The black circle indicates the fiber surface.

Fig. 6 shows the components of the standing wave of $HE_{11}^y$for $a = 300$nm and $\lambda = 800$nm as in the case of the mode profiles in the previous section. The position of the emitter is taken as the 0 degree position ($x = 0$,$y = -a$) and the field is calculated at this position. It is intriguing to note that the z-component of the standing wave is exactly out of phase with the y-component. This is a consequence of the 90 degree complex phase difference seen in the definition of the E_x and E_y components of the HE_{11}mode with respect to the z-component which is seen in Eqs. 7 and 10 as a factor of i in the radial and theta components. Due to the halving of the wavelength induced by the standing wave, this 90 degree phase difference in the travelling wave modes becomes a full 180 degree phase difference between the standing wave fields.

This fact has an important consequence for our experiment. Namely, since our emitters are randomly polarized, even when the emitter is away from the cavity center and thus away from the maximum of the transverse cavity component, it will couple to the longitudinal component which *increases* away from the cavity center. This means that for *any* placement along the fiber axis, we expect to see some coupling to the cavity.

IV. COMPARISON OF FDTD CALCULATED FIELD PROFILES ALONG THE FIBER AXIS WITH FDTD CALCULATED DIPOLE EMITTER TRANSMISSIONS AND PURCELL FACTORS

We now check the results of the previous section against FDTD simulation results for both an HE_{11}^ymode injected into the cavity and for y and z polarized dipole sources coupled to the cavity. We use the following notation:

- Γ_0 - natural decay rate for the dipole emitter in free space.
- Γ_y - Total decay rate of a y-polarized dipole emitter in the presence of the PhC nanofiber.
- Γ_z - Total decay rate of a z-polarized dipole emitter in the presence of the PhC nanofiber.
- $\Gamma_{g,y}$ - Total decay rate into the guided modes of the PhC nanofiber for a y polarized dipole.
- $\Gamma_{g,z}$ - Total decay rate into the guided modes of the PhC nanofiber for a z polarized dipole.

The results shown in Figs. 7, 8, and 9 are for a HE_{11}^ymode injected into the cavity (PhC nanofiber) and for y and z ploarized dipoles placed in the 0 degree position 10 nm the nanofiber surface.

Appendix A: HE_{11}^xfield modes

Figs. 10, 11 and 12 show the intensity of the components of the HE_{11}^xmode for $a = 0.3$ μm, and $\lambda = 800$ nm.

[1] Jelena Vuckovic, "Quantum optics and cavity QED with quantum dots in photonic crystals" http://arxiv.org/abs/1402.2541 .
[2] Katsunari Okamoto "Fundamentals of optical waveguides" Academic Press (2000).
[3] F. L. Kien, J.Q. Liang, K. Hakuta and V.I. Balykin, Opt. Comm. **242**, 445 (2004).

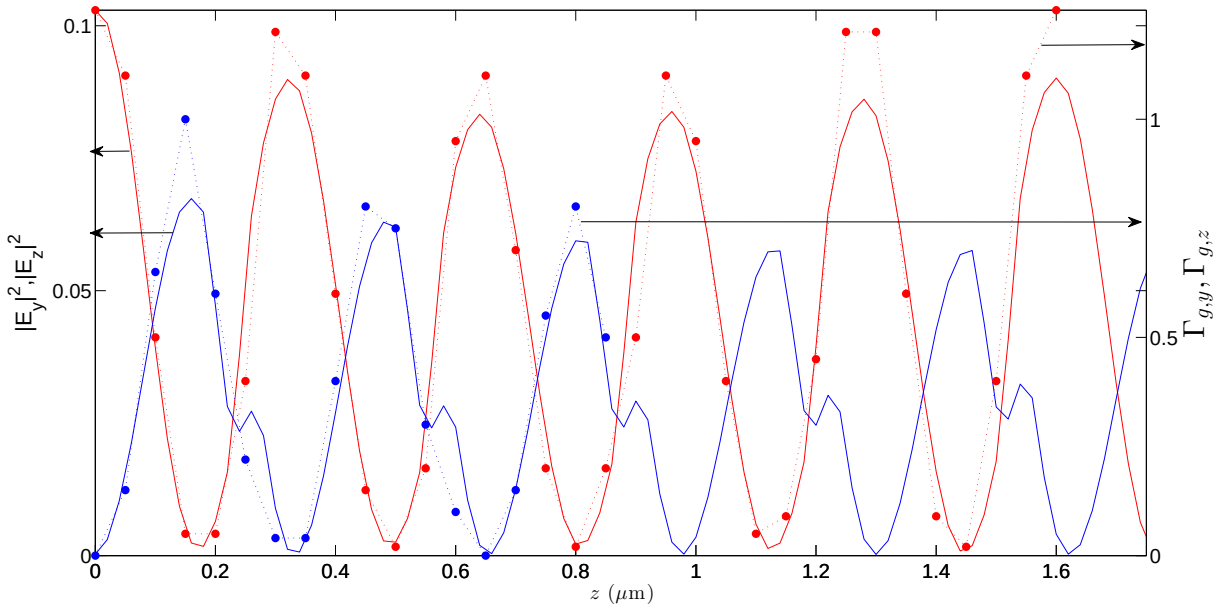

FIG. 7. Solid lines show field intensities $|E_y|^2$ (red line) and $|E_z|^2$ (blue line) for an HE_{11}^y mode injected into the PhC nanofiber. Red dots show y-polarized dipole "transmission" (i.e. Γ_g) and blue dots the z polarized transmission for a dipole placed in the zero degrees position. at the zero

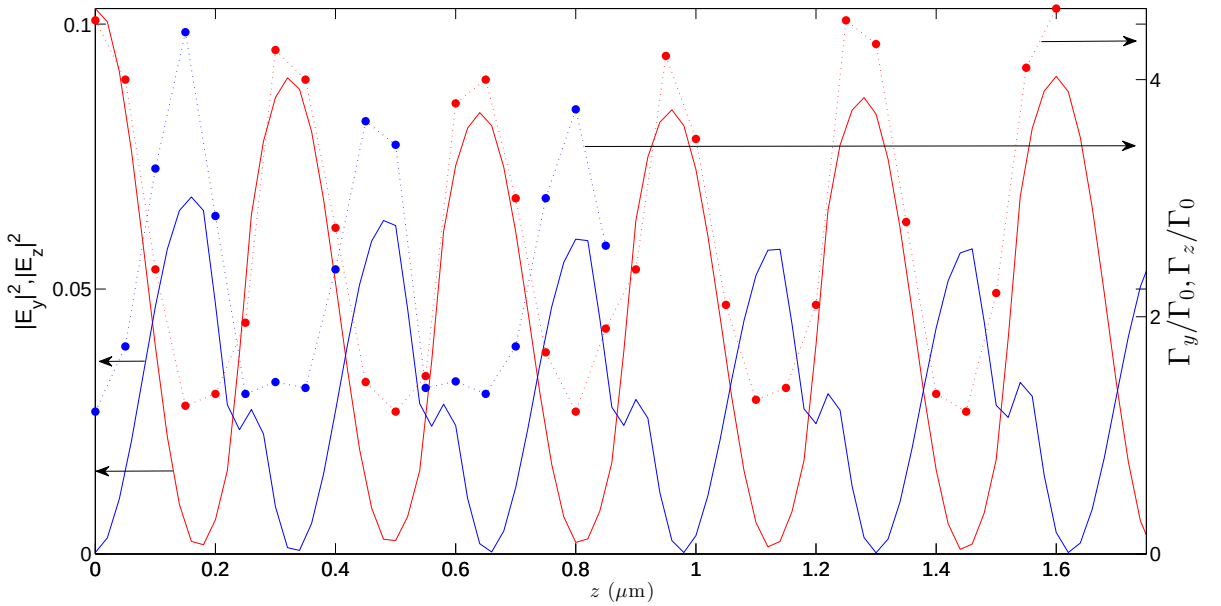

FIG. 8. Solid lines show field intensities $|E_y|^2$ (red line) and $|E_z|^2$ (blue line) for an HE_{11}^y mode injected into the PhC nanofiber. Red dots show y-polarized dipole Purcell factor (i.e. Γ_y/Γ_0) and blue dots the z polarized Purcell factor (Γ_z/Γ_0) for a dipole placed in the zero degrees position.

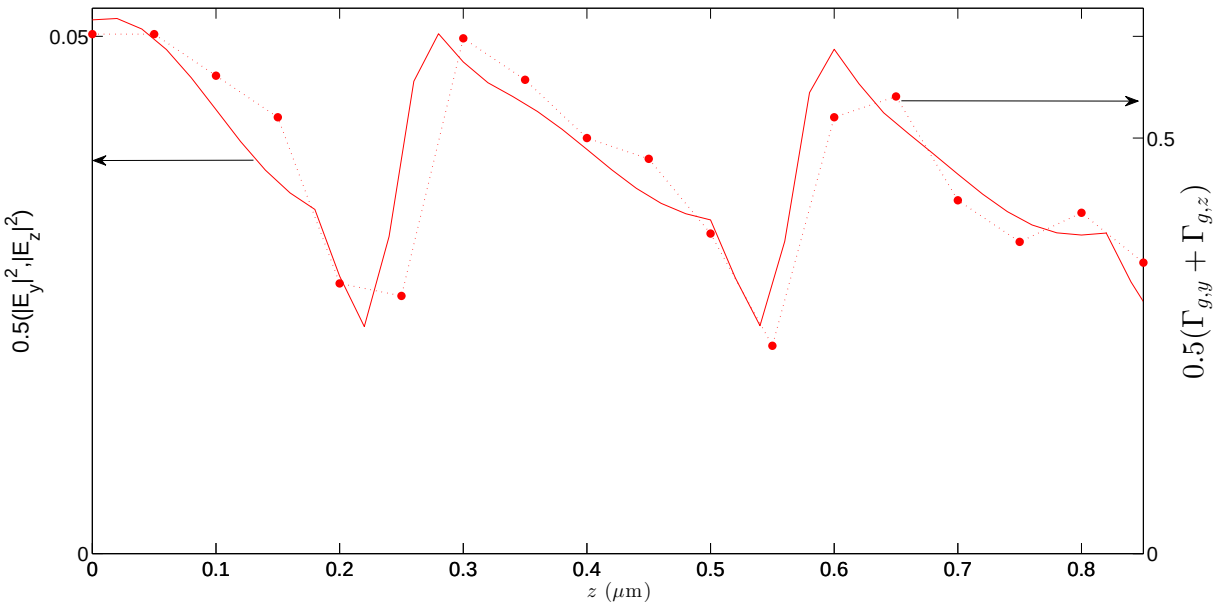

FIG. 9. Averaged intensity of the y and z field intensities (solid line) along with averaged transmission for y and z polarized dipole emitters (points).

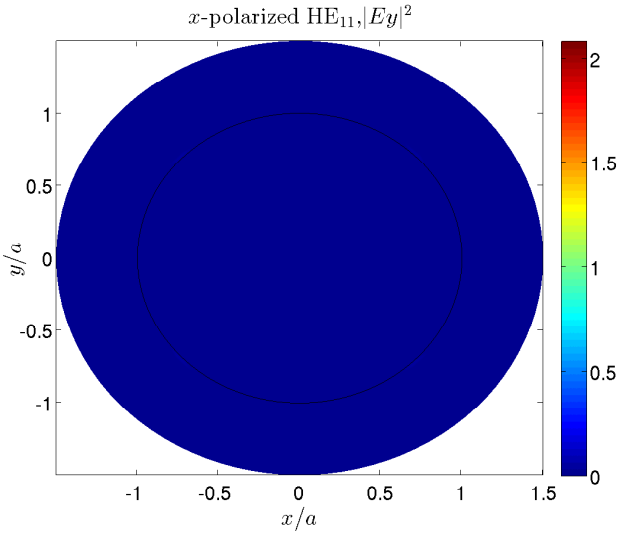

FIG. 10. Intensity of the y components of HE_{11}^{x}. The black circle indicates the fiber surface.

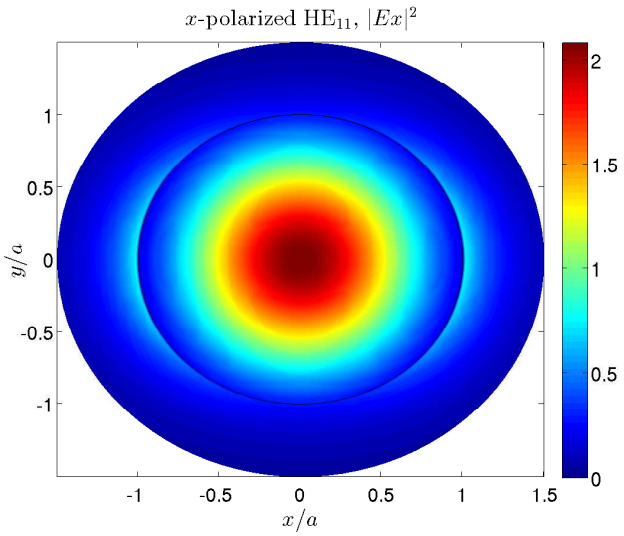

FIG. 11. Intensity of the x components of HE_{11}^{x}.

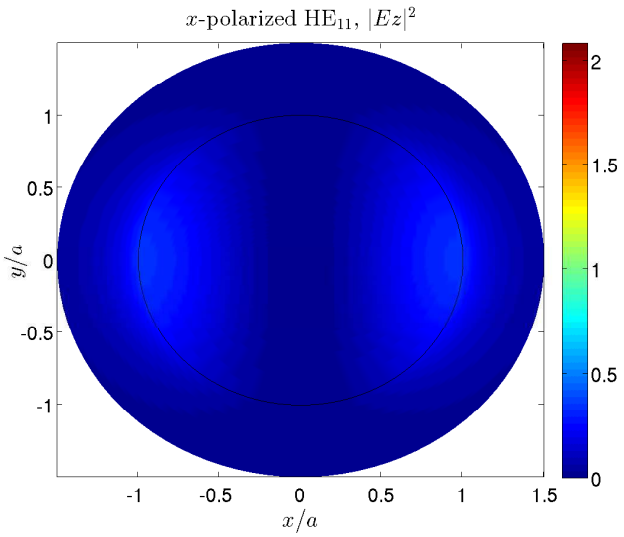

FIG. 12. Intensity of the z components of HE_{11}^{x}.